

## Low-lying states of ruthenium isotopes within the nucleon pair approximation

H. Jiang,<sup>1,2,3,\*</sup> B. Li,<sup>1</sup> and Y. Lei<sup>4</sup>

<sup>1</sup>*School of Arts and Sciences, Shanghai Maritime University, Shanghai 201306, China*

<sup>2</sup>*Shanghai Key Laboratory of Particle Physics and Cosmology and Department of Physics and Astronomy, Shanghai Jiao Tong University, Shanghai 200240, China*

<sup>3</sup>*RIKEN Nishina Center, RIKEN, 2-1 Hirosawa, Wako-shi, Saitama 351-0198, Japan*

<sup>4</sup>*Key Laboratory of Neutron Physics, Institute of Nuclear Physics and Chemistry, China Academy of Engineering Physics, Mianyang 621900, China*

(Received 29 August 2015; revised manuscript received 16 April 2016; published 24 May 2016)

Low-lying states of even-even and odd-mass ruthenium isotopes with mass numbers from 95 to 102, including level schemes, electric quadrupole and magnetic dipole moments, and  $E2$  transition rates, are studied within the framework of the nucleon pair approximation (NPA) of the shell model, by using the phenomenological pairing plus quadrupole interactions. Good agreement is obtained between the calculated results and experimental data. The interesting behaviors of  $g(J_1^+)$  factors versus nuclear spin  $J$  (and mass number  $A$ ) in even-even  $^{96-102}\text{Ru}$  nuclei are analyzed. The dominant configurations of yrast low-lying states in odd-mass  $^{95-101}\text{Ru}$  isotopes are discussed in the collective nucleon-pair subspace. The calculated electric quadrupole moments and magnetic moments of low-lying states, many of which have not yet been measured for these nuclei, are useful for future studies.

DOI: [10.1103/PhysRevC.93.054323](https://doi.org/10.1103/PhysRevC.93.054323)

### I. INTRODUCTION

In recent years many experimental and theoretical efforts have been made in studies of structural and decay properties of nuclei with proton numbers from 28 to 50 [1]. In this region, neutron-rich ruthenium isotopes have attracted much attention for their interesting features in the collectivity evolution [2–21].

Experimental energies of the first  $2^+$  states in even-even  $^{96-114}\text{Ru}$  show a decrease with neutron number up to  $N = 64$ , and become nearly constant around the mid-shell [2]. Spectroscopic studies suggested that the low-lying spectra of  $^{96-104}\text{Ru}$  and  $^{106-114}\text{Ru}$  are vibrational and quasirotational, respectively, and a shape transition was conjectured to arise around  $^{104}\text{Ru}$  based on the systematics of experimental  $B(E2: 2_1^+ \rightarrow 0_1^+)$  values [3]. The low-lying states of even-even Ru isotopes with  $N > 70$  exhibit features associated with triaxial  $\gamma$ -soft deformation in  $^{116,118}\text{Ru}$ , and approach spherical structure with increasing neutron number toward the  $N = 82$  shell closure [4].

The odd-mass ruthenium isotopes around  $A = 100$  are complex and are characterized by both rotational and vibrational types of nuclear excitations [5,6]. Transfer reactions [7] show that the  $5/2_1^+$  and  $7/2_1^+$  states in  $^{97-105}\text{Ru}$  have a quasiparticle character, while the very-low-lying  $3/2_1^+$  states in these nuclei are supposed to be the lowest state of a coexisting configuration.

Magnetic moments of low-lying states are sensitive to nuclear wave functions, thus providing us with an effective probe to study the nuclear structure [22,23]. The measured  $g$  factors of the first  $2^+$  states [denoted by  $g(2_1^+)$ ] in even-even  $^{96-104}\text{Ru}$  isotopes show a gradual decrease with

neutron number [8–13], with values close to the predicted ones of collective model, i.e.,  $g = Z/A$  [24]. For the nuclei  $^{106-112}\text{Ru}$ , the experimental  $g(2_1^+)$  factors show a minimum at  $N \simeq 64$ , the depth of which is difficult to evaluate due to large errors [8,9,17]. The measurements and theoretical explanations of  $g$  factors with nuclear spin  $J > 2$  in this region are challenging for experiments. So far the  $g(4_1^+)$  value in this region is experimentally known for  $^{96}\text{Ru}$  [14],  $^{100}\text{Pd}$  [25], and  $^{106}\text{Pd}$  [26]. The trend of experimental  $g$  factors in these nuclei shows an increase with increasing  $J$ , namely  $g(4_1^+) > g(2_1^+)$ .

A number of theoretical studies of  $g(2_1^+)$  factors have been carried out in the lighter nuclei of Ru isotopes, e.g., the interacting boson model (IBA-2) calculations for  $^{96-114}\text{Ru}$  [8,17], the projected shell model (PSM) calculations for  $^{100-112}\text{Ru}$  [3], the tidal-wave model (TWM) calculations for  $^{96-112}\text{Ru}$  [9], and the shell model (SM) calculations for  $^{96}\text{Ru}$  [14–16]. However, few theoretical studies predicted  $g(4_1^+)$  factors of even-even nuclei in this region. Furthermore, among these works, the TWM calculations [9] predicted  $g(4_1^+) < g(2_1^+)$  for  $^{100-110}\text{Ru}$ ; the SM studies [14,15] predict  $g(4_1^+) < g(2_1^+)$  for  $^{96}\text{Ru}$ . These predictions are not consistent with experimental data.

The purpose of this work is to apply the nucleon pair approximation (NPA) [27] of the shell model to study low-lying structures in even-even  $^{96-102}\text{Ru}$  and odd-mass  $^{95-101}\text{Ru}$  isotopes, especially magnetic moments (or  $g$  factors) of low-lying states. The NPA has been proved to be successful in studying the low-lying states of even-even, odd- $A$ , and odd-odd nuclei in the  $A \sim 80$  [28], 100 [29], 130 [30], and 210 [31] regions. In this model, the dimension of the collective nucleon-pair subspace is small, thus providing a simple and illuminating picture of the structure of the nuclei under investigation. For a recent review, see Ref. [32]. We will show below that in our calculations  $g(2_1^+) < g(4_1^+) < g(6_1^+)$  in even-even  $^{96-102}\text{Ru}$ . This behavior is originated from the contributions of proton-hole configurations.

\*Corresponding author: [huijiang@shmtu.edu.cn](mailto:huijiang@shmtu.edu.cn)

## II. THEORETICAL FRAMEWORK

In the NPA, a collective pair with angular momentum  $r$  and projection  $M$  is defined as [27]

$$A_{M\sigma}^{(r)\dagger} = \sum_{j\sigma j'_\sigma} y(j\sigma j'_\sigma r) (C_{j\sigma}^\dagger \times C_{j'_\sigma}^\dagger)_M^{(r)},$$

where  $C_{j\sigma}^\dagger$  is the single-particle creation operator in the  $j$  orbit, and  $\sigma = \pi$  and  $\nu$  is the index of proton and neutron degrees of freedom, respectively.  $r = 0, 2$  corresponds to  $S$  and  $D$  pairs. The numbers  $y(j\sigma j'_\sigma r)$  are the so-called structure coefficients of the nucleon pair with spin  $r$ .

The NPA Hamiltonian is chosen to have the form

$$\begin{aligned} H = & \sum_{j\sigma} \epsilon_{j\sigma} C_{j\sigma}^\dagger C_{j\sigma} \\ & + \sum_{\sigma} (G_{0\sigma} \mathcal{P}_{\sigma}^{(0)\dagger} \cdot \mathcal{P}_{\sigma}^{(0)} + G_{2\sigma} \mathcal{P}_{\sigma}^{(2)\dagger} \cdot \mathcal{P}_{\sigma}^{(2)}) \\ & + \sum_{\sigma} \kappa_{\sigma} Q_{\sigma} \cdot Q_{\sigma} + \kappa_{\pi\nu} Q_{\pi} \cdot Q_{\nu}, \end{aligned}$$

where  $\epsilon_{j\sigma}$  is the single-particle energy,  $G_{0\sigma}$ ,  $G_{2\sigma}$ ,  $\kappa_{\sigma}$  and  $\kappa_{\pi\nu}$  are the two-body interaction strengths corresponding to monopole, quadrupole pairing and quadrupole-quadrupole interactions between all valence nucleons. The pairing and quadrupole operators are defined as follows.

$$\begin{aligned} \mathcal{P}_{\sigma}^{(0)\dagger} &= \sum_{j\sigma} \frac{\sqrt{2j_{\sigma} + 1}}{2} (C_{j\sigma}^\dagger \times C_{j\sigma}^\dagger)_0^{(0)}, \\ \mathcal{P}_{\sigma}^{(2)\dagger} &= \sum_{j\sigma j'_\sigma} q(j\sigma j'_\sigma) (C_{j\sigma}^\dagger \times C_{j'_\sigma}^\dagger)_M^{(2)}, \\ Q_{\sigma} &= \sum_{j\sigma j'_\sigma} q(j\sigma j'_\sigma) (C_{j\sigma}^\dagger \times \tilde{C}_{j'_\sigma}^\dagger)_M^{(2)}, \end{aligned}$$

where

$$q(jj') = \frac{\Delta_{jj'} (-)^{l+l'+1} (-)^{j-\frac{1}{2}} \hat{j} \hat{j}'}{\sqrt{20\pi}} C_{j\frac{1}{2}, j'-\frac{1}{2}}^{20} \langle nl|r^2|nl' \rangle,$$

with  $\Delta_{jj'} = \frac{1}{2}[1 + (-)^{l+l'+2}]$  and  $C_{j\frac{1}{2}, j'-\frac{1}{2}}^{20}$  is the Clebsch-Gordan coefficient.

The single-particle energies and two-body interaction parameters in our calculations are shown in Table I. Here

TABLE I. Single-particle energies  $\epsilon_{j\sigma}$  (in MeV) and two-body interaction parameters  $G_{0\sigma}$ ,  $G_{2\sigma}$ ,  $\kappa_{\sigma}$ , and  $\kappa_{\pi\nu}$  for proton holes and neutrons. The unit of  $G_{0\sigma}$  is MeV; the units of  $G_{2\sigma}$ ,  $\kappa_{\sigma}$ , and  $\kappa_{\pi\nu}$  are MeV/ $r_0^4$ ;  $r_0^2 = 1.012A^{1/3}$  fm<sup>2</sup>.  $\sigma = \pi, \nu$  stands for proton and neutron, respectively.

$j$	$p_{1/2}$	$p_{3/2}$	$f_{5/2}$	$g_{9/2}$		
$\epsilon_{j\pi}$	0.931	0.702	1.963	0.000		
$j$	$s_{1/2}$	$d_{3/2}$	$d_{5/2}$	$g_{7/2}$	$h_{11/2}$	
$\epsilon_{j\nu}$	1.550	1.660	0.000	0.172	3.550	
$G_{0\nu}$	$G_{2\nu}$	$\kappa_{\nu}$	$G_{0\pi}$	$G_{2\pi}$	$\kappa_{\pi}$	$\kappa_{\pi\nu}$
-0.18	-0.0315	-0.0225	-0.20	-0.040	-0.0225	+0.09

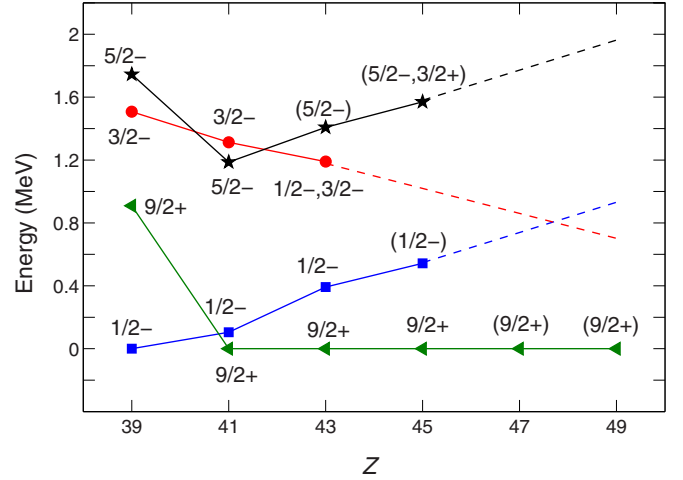


FIG. 1. Systematics of the yrast low-lying energy levels for neutron number  $N = 50$  isotones with odd proton number  $Z$  from 39 to 49. The experimental data (represented by solid symbols) are from Ref. [33]. Extrapolation (dashed lines) to proton-hole single-particle energies is obtained by using linear polynomial fitting of experimental data for each set of levels with  $Z$  from 41 to 45.

the nucleus  $^{100}\text{Sn}$  is taken as the inert core. The neutron single-particle energies  $g_{7/2}$  and  $d_{5/2}$  are taken from the experimental excitation energies of  $^{101}\text{Sn}$  [33]. There are no experimental data for the remaining orbits, and we take those neutron single-particle energies from a previous shell model calculation [34]. The proton-hole single-particle energy  $g_{9/2}$  is also extracted from the corresponding experimental excitation energies of  $^{99}\text{In}$  [33]. Other proton-hole single-particle energies in this table are obtained by extrapolated from the corresponding experimental excited energies of odd-mass  $N = 50$  isotones with  $Z$  from 41 to 45 as shown in Fig. 1. The obtained single-particle energy  $p_{1/2} = 0.931$  MeV is close to the one (0.909 MeV) adopted in a previous shell model calculation [25]. The obtained proton-hole  $p_{3/2}$  orbit is located lower than the  $p_{1/2}$  orbit. Numerical experiments show that the calculated results discussed in this paper are not sensitive to the single-particle energies of the proton-hole  $p_{3/2}$  and  $f_{5/2}$  orbits. This is reasonable because proton-hole configurations of these nuclei are essentially given by the  $g_{9/2}$  orbit (see Fig. 5 for details). Further measurements on the levels of  $^{99}\text{In}$  and  $^{97}\text{Ag}$  would be very useful for evaluating the proton-hole single-particle energies in this mass region.

There are totally seven parameters for the two-body interactions:  $G_{0\pi}$ ,  $G_{0\nu}$ ,  $G_{2\pi}$ ,  $G_{2\nu}$ ,  $\kappa_{\pi}$ ,  $\kappa_{\nu}$ , and  $\kappa_{\pi\nu}$ . The two strengths  $G_{0\pi}$  and  $G_{0\nu}$  of the monopole interactions in Table I are the same as those of our previous calculations in the  $A \sim 100$  region [29]. The remaining five parameters are obtained by fitting to the experimental excited energies and electromagnetic properties of low-lying states. For the odd-mass nuclei, we assume the same parameters as for their even-even cores.

The  $E2$  transition operator is defined by  $T(E2) = e_{\pi} Q_{\pi} + e_{\nu} Q_{\nu}$ , where  $e_{\pi}$  and  $e_{\nu}$  are the effective charges of valence proton-holes and neutrons, respectively. The  $B(E2)$  value in

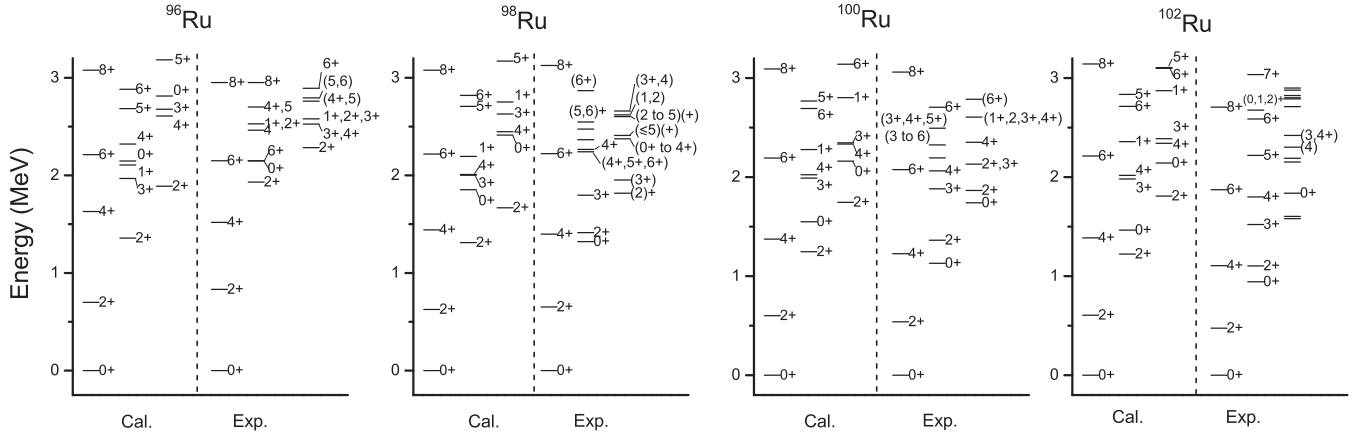


FIG. 2. Partial low-lying states in even-even  $^{96-102}\text{Ru}$  isotopes. Experimental data are taken from Ref. [33].

units of W.u. is given by

$$B(E2; J_i \rightarrow J_f) = \frac{2J_f + 1}{2J_i + 1} \times \frac{(e_\pi \chi_\pi + e_\nu \chi_\nu)^2 r_0^4}{5.94 \times 10^{-6} \times A^{4/3}},$$

with reduced matrix element  $\chi_\sigma = \langle \beta_f, J_f || Q_\sigma || \beta_i, J_i \rangle$  ( $\sigma = \pi, \nu$ ) and  $r_0^2 = 1.012A^{1/3} \text{ fm}^2$ .  $|\beta_i, J_i\rangle$  is the eigenfunction of  $J_i$  state. Our neutron effective charge is taken to be  $e_\nu = 1.28e$ , the same as for tin isotopes [29]. The proton-hole effective charge  $e_\pi = -1.98e$  is obtained by fitting to the experimental data. The electric quadrupole moment (in units of  $eb$ ) is

$$Q(J_i) = \sqrt{\frac{16\pi}{5}} C_{J_i J_i, 20}^{J_i J_i} (e_\pi \chi_\pi + e_\nu \chi_\nu) r_0^2.$$

The magnetic dipole moment is defined by

$$\mu(J_i) = C_{J_i J_i, 10}^{J_i J_i} (T_\pi + T_\nu) \mu_N,$$

with reduced matrix element  $T_\sigma = \langle \beta_i, J_i || g_{l\sigma} L_\sigma + g_{s\sigma} S_\sigma || \beta_i, J_i \rangle$  ( $\sigma = \pi, \nu$ ). Here,  $\mu_N$  is the nuclear magneton.  $L_\sigma$  and  $S_\sigma$  are the orbital and spin angular momenta, and  $g_{l\sigma}$  and  $g_{s\sigma}$  are the orbital and spin gyromagnetic ratios, respectively. The  $g$  factor is defined by  $\frac{\mu(J_i)/\mu_N}{J_i}$ . In the above convention of unit, the  $g$  factors,  $L_\sigma$ ,  $S_\sigma$ , and  $J_i$  are dimensionless. The effective spin gyromagnetic ratios are taken to be  $g_{s\pi} = 3.18$  and  $g_{s\nu} = -2.18$ , which are from previous shell model calculations for the same nuclear region [14, 16, 35]. Namely, the quenching factor of 0.57 for spin gyromagnetic ratios is used. Three sets of orbital gyromagnetic ratios are used in this paper. In the first set we use the bare ones  $g_{l\pi} = 1$  and  $g_{l\nu} = 0$ . In the second set, we take  $g_{l\pi} = 0.94$  and  $g_{l\nu} = 0.07$ , which are the optimized parameters determined by  $\chi^2$  fitting of experimental  $\mu$  values for both even-even and odd-mass nuclei. In the last set, we use the conventional effective values  $g_{l\pi} = 1.1$  and  $g_{l\nu} = -0.1$  [23]. For convenience we denote them by NPA-1, NPA-2, and NPA-3, respectively.

Our model space is constructed by  $SD$  pairs of valence neutron and proton-holes with respect to the nucleus  $^{100}\text{Sn}$ , by considering the vibrational structure of the nuclei studied here. We have also made comparisons of excited energies,  $g$  factors, and  $B(E2)$  strengths calculated under different

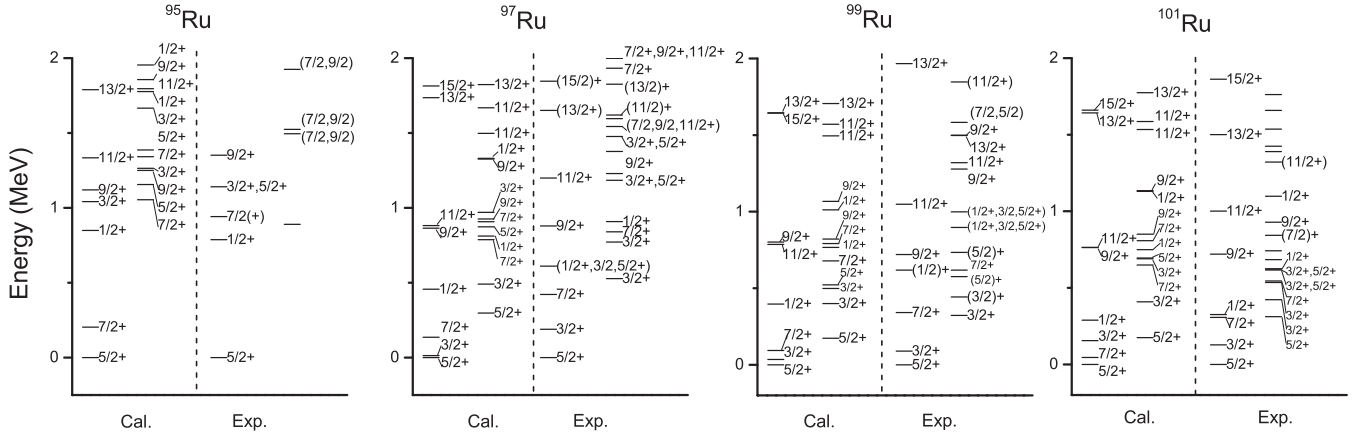
configuration subspaces. It is shown that the calculation in expanded nucleon-pair subspace with the inclusion of higher-spin pairs does not improve our calculated results essentially. The structure coefficients of even-even nuclei are obtained based on a variational procedure as in Ref. [31]. The structure coefficients of odd-mass nuclei are taken to be the same as those of their even-even cores.

### III. CALCULATIONS AND DISCUSSIONS

In this section, we present calculated low-lying energy levels,  $E2$  transition strengths, electric quadrupole moments  $Q$ , and magnetic dipole moments  $\mu$  (or  $g$  factors) in Figs. 2 and 3 and Tables II and III, for even-even  $^{96-102}\text{Ru}$  and odd-mass  $^{95-101}\text{Ru}$  isotopes, respectively, with a comparison of corresponding experimental data. A reasonably good agreement is obtained for yrast states. This shows that the NPA provides an appropriate theoretical framework to describe low-lying states of these nuclei.

Let us first come to even-even cases. The energy ratio of the first  $4^+$  state with respect to the first  $2^+$  state, namely  $R_{4/2} = E(4_1^+)/E(2_1^+)$ , is a well known observable of the extent of quadrupole deformation [4]. It is known that  $R_{4/2} = 2.0$  for a harmonic vibrator  $U(5)$ ,  $R_{4/2} = 2.5$  for  $\gamma$ -unstable  $O(6)$ , and  $R_{4/2} = 3.33$  for an axially symmetric rotor  $SU(3)$ . In Fig. 2, the experimental  $R_{4/2}$  is equal to 1.82, 2.14, 2.27, and 2.33 for  $^{96, 98, 100, 102}\text{Ru}$ , respectively. This indicates that even-even  $^{96-102}\text{Ru}$  isotopes are around  $U(5)$  character, exhibiting a gradually increasing deformation away from the spherical structure as neutron number moves away from the  $N = 50$  closed shell.

The structures of non-yrast states in these even-even nuclei are more complicated than those of yrast states. One sees in Fig. 2 that the agreement for these low-lying non-yrast states is reasonable except for the  $0_2^+$  level in  $^{98-102}\text{Ru}$  nuclei, where the calculated  $0_2^+$  levels are systematically higher than experimental values. We have tried to describe this state by expanding our configurations in the shells of Table I, i.e., further considering other possible pairs. Unfortunately, the improvement along this line is not encouraging. This systematic deviation is warranted for future studies.

FIG. 3. Same as Fig. 2 except for odd-mass  $^{95-101}\text{Ru}$  isotopes.

Now let us focus on our predicted electromagnetic reduced transition properties of yrast states in these nuclei. One sees in Table II that  $|Q(2_1^+)|$ ,  $B(E2: 2_1^+ \rightarrow 0_1^+)$ , and  $B(E2: 4_1^+ \rightarrow 2_1^+)$  values are predicted to increase with  $N$  in our calculations. The experimental  $Q(2_1^+)$  values in  $^{98-102}\text{Ru}$  are strongly affected by the sign of the second order interference term arising from the direct excitation of the first  $2_1^+$  level and the excitation through a higher lying intermediate  $2^+$

state [37]. The corresponding experimental values in Table II are  $-0.20(9)$ ,  $-0.54(7)$ , and  $-0.64(5)$  for positive sign [and  $-0.01(9)$ ,  $-0.33(7)$ , and  $-0.33(4)$  for negative sign] for the interference terms in  $^{98,100,102}\text{Ru}$ , respectively. One sees in this table that our results agree with the measured value based on the positive sign for  $^{98}\text{Ru}$ , while for  $^{100,102}\text{Ru}$  our calculations favor the negative sign. Further experimental measurements are therefore necessary for these states.

TABLE II.  $B(E2)$  values (in units of W.u.), electric quadrupole moments  $Q$  (in units of  $eb$ ), and  $g$  factors for even-even  $^{96-102}\text{Ru}$  with the comparison between experimental data and the results in this work. Experimental  $B(E2)$  and  $Q$  values are taken from Ref. [33] and [36], respectively. For measured  $Q(2_1^+)$  values in  $^{98-102}\text{Ru}$ , the left (right) values are based on the positive (negative) sign of the interference term, respectively [37]. For  $B(E2: 4_1^+ \rightarrow 2_1^+)$  in  $^{98}\text{Ru}$ , we also list other measured values from <sup>a</sup> Ref. [38,39], <sup>b</sup> Ref. [40], and <sup>c</sup> Ref. [41]. Experimental  $g$  factors in this table are from <sup>d</sup> Ref. [9] and <sup>e</sup> Ref. [14]. There are also some other experimental  $g(2_1^+)$  factors in the last few years and we list them as follows:  $g(2_1^+) = 0.47(3)$  [10] and  $0.46(2)$  [14] for  $^{96}\text{Ru}$ ;  $0.47(3)$  [10] and  $0.4(3)$  [11] for  $^{98}\text{Ru}$ ;  $0.44(3)$  [10] and  $0.48(6)$  [12] for  $^{100}\text{Ru}$ ; and  $0.43(3)$  [10] and  $0.36(3)$  [13] for  $^{102}\text{Ru}$ . For the orbital gyromagnetic ratios, we adopt the values  $g_{l\pi} = 1$  and  $g_{lv} = 0$  in NPA-1,  $g_{l\pi} = 0.94$  and  $g_{lv} = 0.07$  in NPA-2, and  $g_{l\pi} = 1.1$  and  $g_{lv} = -0.1$  in NPA-3.

Nuclei	State		$B(E2: J_i^\pi \rightarrow J_f^\pi)$		$Q(J_i^\pi)$		$g(J_i^\pi)$			
	$J_i^\pi$	$J_f^\pi$	Expt.	NPA	Expt.	NPA	Expt.	NPA-1	NPA-2	NPA-3
$^{96}\text{Ru}$	$2_1^+$	$0_1^+$	18.4(4)	21.61	$-0.13(9)$	$-0.15$	$0.445(28)^d$	0.41	0.44	0.38
	$4_1^+$	$2_1^+$	20.7(15)	22.06		$-0.13$	$0.58(8)^e$	0.98	0.95	1.03
	$6_1^+$	$4_1^+$	14(5)	18.01		$-0.51$		1.11	1.06	1.18
	$2_2^+$	$2_1^+$	18.4(24)	7.44		$+0.11$		0.86	0.84	0.89
	$2_2^+$	$0_1^+$		2.39						
$^{98}\text{Ru}$	$2_1^+$	$0_1^+$	32(5)	30.86	$-0.20(9)$ or $-0.01(9)$	$-0.25$	$0.408(32)^d$	0.41	0.44	0.38
	$4_1^+$	$2_1^+$	12(3)/40(5) <sup>e</sup>	40.64		$-0.34$		0.59	0.60	0.58
			50(18) <sup>b</sup> /57.6(40) <sup>c</sup>							
	$6_1^+$	$4_1^+$	12.9(15)	28.47		$-0.57$		0.97	0.94	1.02
	$2_2^+$	$2_1^+$	45(16)	27.47		$+0.16$		0.58	0.59	0.57
$^{100}\text{Ru}$	$2_2^+$	$0_1^+$	1.0(4)	1.48						
	$2_1^+$	$0_1^+$	35.6(4)	36.88	$-0.54(7)$ or $-0.33(7)$	$-0.31$	$0.429(23)^d$	0.43	0.46	0.39
	$4_1^+$	$2_1^+$	51(4)	52.27		$-0.48$		0.53	0.55	0.51
	$6_1^+$	$4_1^+$	$< 1.7 \times 10^2$	46.75		$-0.64$		0.80	0.79	0.82
	$2_2^+$	$2_1^+$	30.9(4)	38.21		$+0.18$		0.49	0.51	0.46
$^{102}\text{Ru}$	$2_2^+$	$0_1^+$	$1.9^{(+4)}_{(-5)}$	1.62						
	$2_1^+$	$0_1^+$	44.6(7)	40.33	$-0.64(5)$ or $-0.33(4)$	$-0.30$	$0.453(23)^d$	0.46	0.48	0.42
	$4_1^+$	$2_1^+$	66(11)	58.21		$-0.52$		0.55	0.57	0.53
	$6_1^+$	$4_1^+$	68(25)	56.39		$-0.71$		0.75	0.74	0.77
	$2_2^+$	$2_1^+$	(32)(5)	46.14		$+0.16$		0.46	0.49	0.43
	$2_2^+$	$0_1^+$	1.14(15)	1.62						

TABLE III.  $B(E2)$  values (in units of W.u.), electric quadrupole moments  $Q$  (in units of  $eb$ ) and magnetic moments  $\mu$  (in units of  $\mu_N$ ) for odd-mass  $^{95-101}\text{Ru}$  isotopes. Experimental data are from Refs. [33,36].

Nuclei	State		$B(E2 : J_i^\pi \rightarrow J_f^\pi)$		$Q(J_i^\pi)$		$\mu(J_i^\pi)$			
	$J_i^\pi$	$J_f^\pi$	Expt.	NPA	Expt.	NPA	Expt.	NPA-1	NPA-2	NPA-3
$^{95}\text{Ru}$	$5/2_1^+$					-0.36	(- )0.861(7)	-0.97	-0.83	-1.16
	$3/2_1^+$	$5/2_1^+$		8.31		-0.15		+0.12	+0.26	-0.07
	$7/2_1^+$	$5/2_1^+$		1.13		-0.42		+0.93	+1.20	+0.55
	$17/2_1^+$	$13/2_1^+$	6.4(6)	9.32		-0.60	+6.98(14)	+6.26	+6.06	+6.59
	$11/2_2^+$	$7/2_1^+$	0.0122(5)	0.05		-0.09		+3.77	+3.66	+3.95
$^{97}\text{Ru}$	$5/2_1^+$					-0.08	(- )0.787(8)	-0.85	-0.71	-1.03
	$3/2_1^+$	$5/2_1^+$	30(12)	27.78		+0.17		-0.48	-0.40	-0.59
	$7/2_1^+$	$5/2_1^+$	0.012(4)	0.85		-0.34		+0.95	+1.22	+0.58
	$11/2_1^+$	$7/2_1^+$	9(6)	23.18		-0.47		+1.75	+2.08	+1.32
	$15/2_1^+$	$11/2_1^+$	14.9(17)	22.74		-0.38		+5.06	+5.18	+4.93
$^{99}\text{Ru}$	$5/2_1^+$				+0.079(4)	+0.19	-0.641(5)	-0.76	-0.62	-0.94
	$3/2_1^+$	$5/2_1^+$	50.1(10)	33.05	+0.231(12)	+0.21	-0.292(3)	-0.40	-0.32	-0.52
	$7/2_1^+$	$5/2_1^+$		1.26		-0.18		+0.96	+1.23	+0.60
	$5/2_2^+$	$5/2_1^+$	11(5)	5.82		+0.06		+0.45	+0.63	+0.21
	$7/2_2^+$	$5/2_1^+$	23(18)	32.34		-0.03		+0.20	+0.34	+0.01
$^{101}\text{Ru}$	$5/2_1^+$				+0.44(2)	+0.37	-0.719(6)	-0.76	-0.63	-0.95
	$3/2_1^+$	$5/2_1^+$	19.9(24)	32.55		+0.14	-0.210(5)	-0.43	-0.34	-0.54
	$7/2_1^+$	$5/2_1^+$	$1.4^{(+15)}_{(-4)}$	0.40		+0.01		+0.95	+1.22	+0.58
	$7/2_1^+$	$3/2_1^+$	13(4)	3.26						
	$7/2_2^+$	$5/2_1^+$	$1.3 \times 10^2(3)$	42.37		+0.06		+0.16	+0.31	-0.02

$^{98}\text{Ru}$  is an intriguing nucleus [38–43]. On the one hand, it is a light ruthenium isotope close to the  $N = 50$  shell closure with  $R_{4/2} = 2.14$  and  $B(E2 : 2_1^+ \rightarrow 0_1^+) = 32(5)$  W.u. [33]. On the other hand, there are noticeable differences in magnitudes for  $B(E2 : 4_1^+ \rightarrow 2_1^+)$  strengths obtained in different experiments. A recoil-distance lifetime measurement in 1999 [43] yielded the most precise value with  $B(E2 : 4_1^+ \rightarrow 2_1^+) = 12(3)$  W.u. and  $B_{4/2} = B(E2 : 4_1^+ \rightarrow 2_1^+)/B(E2 : 2_1^+ \rightarrow 0_1^+) = 0.38(11)$ , indicating a breakdown of vibrational symmetry occurring at  $^{98}\text{Ru}$ . Other lifetime measurements yielded a weak-collective or vibrational value, with  $B(E2 : 4_1^+ \rightarrow 2_1^+) = 40(5)$  W.u. and  $B_{4/2} = 1.41(27)$  in 1980 [39],  $B(E2 : 4_1^+ \rightarrow 2_1^+) = 50(18)$  W.u. and  $B_{4/2} = 1.7(6)$  in 2006 [40], and  $B(E2 : 4_1^+ \rightarrow 2_1^+) = 57.6(40)$  W.u. and  $B_{4/2} = 1.86(16)$  in 2012 [41].

A number of theoretical calculations have been carried out to analyze  $B(E2)$  strengths in  $^{98}\text{Ru}$ . The IBA-1 calculations [41,42] suggested a weakly collective vibrational character up to the two-phonon triplet with  $B_{4/2} = 1.5$ ; however, these calculations predicted  $B(E2 : 6_1^+ \rightarrow 4_1^+)$  strength to be 46 W.u., which is not in agreement with experimental data. The SM calculation [43] predicted weak  $E2$  transitions between  $2_1^+$  and  $0_1^+$ ,  $4_1^+$  and  $2_1^+$ , and  $6_1^+$  and  $4_1^+$ ; their calculated  $B(E2 : 2_1^+ \rightarrow 0_1^+) = 15.37$  W.u. is about half the experimental value. One sees in Table II that the present calculation agrees reasonably well with the corresponding experimental data. Our calculated  $B(E2 : 4_1^+ \rightarrow 2_1^+) = 40.64$  W.u. and  $B_{4/2} = 1.32$ , suggesting the weakly collective vibrational character for the yrast states up to spin 4.

Now we come to  $g$  factors in Table II. The measured  $g(J > 2)$  factors are quite scarce in this mass region. Available experimental  $g(4_1^+)$  factors in  $^{96}\text{Ru}$  [14],  $^{100}\text{Pd}$  [25], and

$^{106}\text{Pd}$  [26] suggest that  $g(4_1^+) > g(2_1^+)$ . One sees in Table II that our results in  $^{96-102}\text{Ru}$  show an increasing trend with  $J$ , namely,  $g(6_1^+) > g(4_1^+) > g(2_1^+)$ . To understand the general trend of  $g$  factors, we analyze the contributions from their proton/neutron spin and orbital angular momentum components as a function of  $A$  and  $J$  presented in Figs. 4(a) and 4(a') and in Figs. 4(b) and 4(b'), respectively, for two sets of orbital

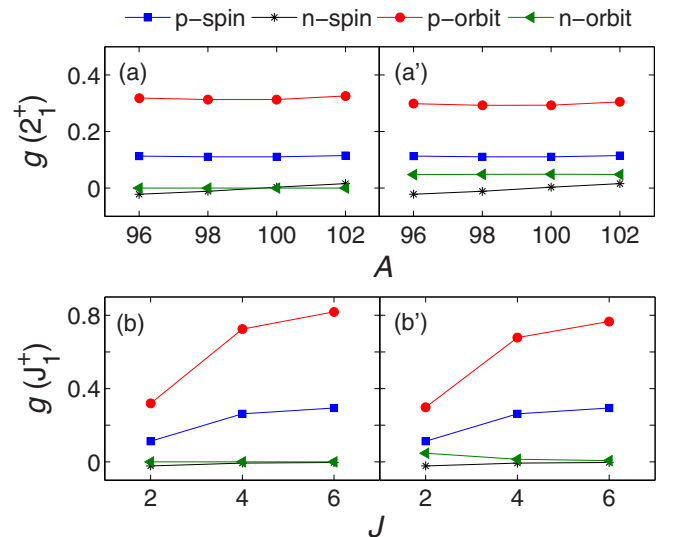


FIG. 4. The proton/neutron spin part and orbital part contributions in the  $g$  factors. Panels (a) and (b) show our calculated  $g(2_1^+)$  factors versus  $A$  and  $g(4_1^+)$  factors versus  $J$  of  $^{96}\text{Ru}$  in the NPA-1, respectively. Panels (a') and (b') show the same as panels (a) and (b) but for the NPA-2.

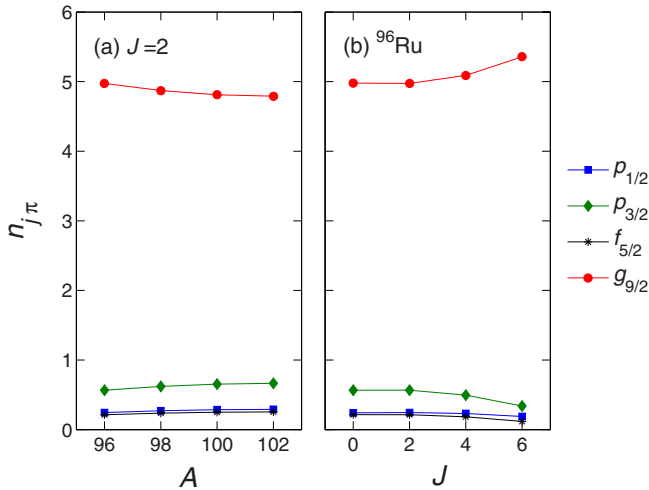


FIG. 5. The expectation value of occupation number  $n_{j\pi}$  in the proton  $p_{1/2}$ ,  $p_{3/2}$ ,  $f_{5/2}$ , and  $g_{9/2}$  orbits. Panel (a): versus mass number  $A$  for the first excited state with spin 2. Panel (b): versus spin  $J$  in  $^{96}\text{Ru}$ .

gyromagnetic ratios. One sees that the overall trend of  $g(2_1^+)$  factors as a function of  $A$  in Fig. 4(a), as well as  $g(J_1^+)$  factors as a function of  $J$  in Fig. 4(b), is mainly determined by the proton part contributions. The neutron part contribution is negligible, because their values are close to zero.

In Fig. 5, we present the expectation value of occupation number  $n_{j\pi}$  in the proton  $p_{1/2}$ ,  $p_{3/2}$ ,  $f_{5/2}$ , and  $g_{9/2}$  orbits, respectively. For Ru isotopes, the proton-hole number is six in our calculation. One sees in Fig. 5 that most proton holes occupy the  $g_{9/2}$  orbit, with expectation values of  $n_{g_{9/2}\pi}$  between 4.8 and 5.5. It is also seen that the  $n_{g_{9/2}\pi}$  values decrease slightly with  $A$  for  $2_1^+$  state, while they show an increase with  $J$  in  $^{96}\text{Ru}$ . The empirical single-particle  $\pi g_{9/2}$  factor is known to be large and positive (its Schmidt value is +1.510) [25]. Therefore the dominant proton character in Fig. 4 is suggested to be related to the proton holes in the  $\pi g_{9/2}$  orbit.

Our predicted  $g(4_1^+)$  factor in  $^{96}\text{Ru}$  is larger than the experimental value, which seems to be robust for different configuration spaces. In the NPA-1, we adopt the bare orbital gyromagnetic ratios, namely,  $g_{l\pi} = 1$  and  $g_{lv} = 0$ . If we adopted  $g_{l\pi} = 0.47$  and  $g_{lv} = 0.16$ , we would obtain good consistency with experimental value for this state; however, such parameters would lead to very large deviation from experimental magnetic moment of the  $17/2_1^+$  state in  $^{95}\text{Ru}$ . Therefore, further measurements on the  $g(4_1^+)$  factor would be very useful to clarify the physics of  $4_1^+$  state in  $^{96}\text{Ru}$ .

Finally we look at our results of odd-mass nuclei shown in Fig. 3 and Table III. Here, we list the magnetic moments  $\mu$  instead of  $g$  factors in Table III.

The structures of odd-mass nuclei are much more complicated than their even-even neighbors. One sees in Fig. 3 that most low-lying states are reasonably well reproduced in our systematic calculations. Our calculated ground states of these nuclei have  $J^\pi = 5/2^+$ , which is consistent with experiments. One also sees deviations for the  $7/2_1^+$  and  $11/2_1^+$  states. We note that such deviations are easily fixed by including the

monopole interaction between valence nucleons, meanwhile the wave functions are essentially the same [44].

It is also interesting to note that three sets of orbital gyromagnetic ratios (NPA-1, NPA-2, and NPA-3) yield similar calculated  $g$  factors of even-even nuclei. On the other hand, if we adopt the conventional effective values ( $g_{l\pi} = 1.1$  and  $g_{lv} = -0.1$ ), as in NPA-3, calculated  $\mu$  values of odd mass nuclei would deviate from the experimental data for a number of states. For example,  $\mu(5/2_1^+)$  of  $^{95}\text{Ru}$  are predicted to be  $-0.83\mu_N$  in NPA-2 and  $-1.16\mu_N$  in NPA-3. Therefore the parametrization of the  $g$  factors in this nuclear region is worthy of further discussion in the future.

To understand structures of yrast low-lying states in these nuclei, we analyze them within our collective nucleon-pair subspace. The dominant NPA configurations corresponding to the  $5/2_1^+$  and  $7/2_1^+$  states are  $|(d_{5/2})_v S_v^{N_v} S_\pi^3\rangle$  and  $|(g_{7/2})_v S_v^{N_v} S_\pi^3\rangle$ , respectively. This indicates that these two levels have an important quasiparticle character in Ru isotopes [7]. Therefore their  $\mu$  values, determined by the unpaired neutron, are nearly invariant in Table III. The  $3/2_1^+$  states of these odd- $A$  Ru isotopes are more complicated than  $5/2_1^+$  and  $7/2_1^+$  states. In Fig. 3, experiments suggest that it locates at about 1 MeV and 0.1–0.2 MeV above the ground state in  $^{95}\text{Ru}$  and  $^{97-101}\text{Ru}$ , respectively. This suggests that the structure of  $3/2_1^+$  state in  $^{95}\text{Ru}$  is different from that in  $^{97-101}\text{Ru}$ . This is indeed the case in our calculations. One sees in Fig. 3 and Table III that our results reasonably reproduced this structural change both in the energy spectrum and  $\mu$  values. Their dominant NPA configurations are found to be  $a|(d_{3/2})_v S_v^{N_v} S_\pi^3\rangle + b|(d_{5/2})_v S_v^{N_v} D_\pi S_\pi^2\rangle + c|(g_{7/2})_v S_v^{N_v} D_\pi S_\pi^2\rangle$  in  $^{95}\text{Ru}$  and  $|(d_{5/2})_v D_v S_v^{N_v-1} S_\pi^3\rangle$  in  $^{97-101}\text{Ru}$ . Our results agree with the conjecture in Ref. [7] that the very-low-lying  $3/2_1^+$  states in  $^{97-101}\text{Ru}$  have a small overlap with the neighboring  $0^+$  ground states plus one quasiparticle.

#### IV. SUMMARY

In this paper we have studied low-lying states of even-even  $^{96-102}\text{Ru}$  and odd-mass  $^{95-101}\text{Ru}$ , with focus on energy levels, electric quadrupole and magnetic dipole moments, and  $E2$  transition rates between low-lying states, within the nucleon pair approximation (NPA) of the shell model. We take the phenomenological pairing plus quadrupole interactions between valence nucleons. The overall agreement between the calculated results and experimental data is good. This indicates that the NPA provides us with an appropriate theoretical framework to study low-lying states of these nuclei, which certainly will be useful when more data are available.

We investigate energy ratio  $R_{4/2}$  and  $B(E2)$  ratio  $B_{4/2}$  in even-even  $^{96-102}\text{Ru}$  isotopes. Our results present the  $U(5)$  characters of low-lying states in these nuclei. Our calculated  $B(E2 : 4_1^+ \rightarrow 2_1^+)$  and  $B_{4/2}$  agree with the weakly collective vibrational character for the yrast states up to spin 4 in  $^{98}\text{Ru}$ .

We study the  $g(2_1^+)$ ,  $g(4_1^+)$ , and  $g(6_1^+)$  factors in these even-even nuclei. Our predicted  $g(J_1^+)$  factors increase with nuclear spin, namely,  $g(2_1^+) < g(4_1^+) < g(6_1^+)$ . We analyze the contribution from the proton/neutron spin part and orbital part contributions in the  $g$  factors. The overall trend of  $g(2_1^+)$  factors as a function of mass number, as well as the  $g(J_1^+)$  factors as

a function of nuclear spin in  $^{96}\text{Ru}$ , are suggested to be given essentially by proton-holes in the  $\pi g_{9/2}$  orbit.

We analyze structures of yrast low-lying states in odd-mass  $^{95-101}\text{Ru}$  within our collective nucleon-pair subspace. The  $5/2_1^+$  (and  $7/2_1^+$ ) states are well represented by the coupling between  $S$  pairs and an unpaired neutron in the  $\nu d_{5/2}$  (and  $\nu g_{7/2}$ ) orbit. We suggest a structural change of  $3/2_1^+$  state in these odd-mass nuclei as mass number moves from 95 to 97.

## ACKNOWLEDGMENTS

This work was supported by the National Natural Science Foundation of China (Grants No. 11305101, No. 11247241, and No. 11305151). H.J. thanks the Program of Shanghai Academic/Technology Research Leader (Grant No. 16XD1401600), and RIKEN Nishina Center for financial support. Discussions with Prof. A. Arima and Prof. Y. M. Zhao are gratefully acknowledged.

- 
- [1] T. Faestermann, M. Górska, and H. Grawe, *Prog. Part. Nucl. Phys.* **69**, 85 (2013), and references therein.
- [2] Y. B. Wang and J. Rissanen, *Hyperfine Interact.* **223**, 167 (2014).
- [3] A. Bhat, A. Bharti, and S. K. Khosa, *Int. J. Mod. Phys. E* **21**, 1250030 (2012).
- [4] P.-A. Söderström *et al.*, *Phys. Rev. C* **88**, 024301 (2013).
- [5] S. Bhattacharya and S. K. Basu, *Phys. Rev. C* **18**, 2765 (1978).
- [6] J. L. M. Duarte, L. B. Horodyski-Matsushigue, T. Borello-Lewin, and O. Dietzsch, *Phys. Rev. C* **38**, 664 (1988).
- [7] T. Borello-Lewin, J. L. M. Duarte, L. B. Horodyski-Matsushigue, and M. D. L. Barbosa, *Phys. Rev. C* **57**, 967 (1998).
- [8] A. G. Smith *et al.*, *J. Phys. G: Nucl. Part. Phys.* **31**, S1433 (2005).
- [9] S. K. Chamoli *et al.*, *Phys. Rev. C* **83**, 054318 (2011).
- [10] M. J. Taylor *et al.*, *Phys. Rev. C* **83**, 044315 (2011).
- [11] B. Singh and Z. Hu, *Nucl. Data Sheets* **98**, 335 (2003).
- [12] B. Singh, *Nucl. Data Sheets* **109**, 297 (2008).
- [13] D. De Frenne, *Nucl. Data Sheets* **110**, 1745 (2009).
- [14] D. A. Torres *et al.*, *Phys. Rev. C* **85**, 017305 (2012).
- [15] P. Halse, *J. Phys. G: Nucl. Part. Phys.* **19**, 1859 (1993).
- [16] J. D. Holt, N. Pietralla, J. W. Holt, T. T. S. Kuo, and G. Rainovski, *Phys. Rev. C* **76**, 034325 (2007).
- [17] A. Giannatiempo, *Eur. Phys. J. A* **49**, 37 (2013).
- [18] J. Kotila, J. Suhonen, and D. S. Delion, *Phys. Rev. C* **68**, 054322 (2003).
- [19] Y. X. Liu and Y. Sun, *J. Phys.: Conf. Ser.* **420**, 012046 (2013).
- [20] F. Ghazi Moradi *et al.*, *Phys. Rev. C* **89**, 014301 (2014).
- [21] A. Hennig *et al.*, *Phys. Rev. C* **90**, 051302(R) (2014).
- [22] N. Benczer-Koller and G. J. Kumbartzki, *J. Phys. G: Nucl. Part. Phys.* **34**, R321 (2007), and references therein.
- [23] K.-H. Speidel, O. Kenn, and F. Nowacki, *Prog. Part. Nucl. Phys.* **49**, 91 (2002), and references therein.
- [24] A. Bohr and B. R. Mottelson, *Nuclear Structure* (Benjamin, New York, 1975).
- [25] D. A. Torres *et al.*, *Phys. Rev. C* **84**, 044327 (2011).
- [26] G. Gürdal *et al.*, *Phys. Rev. C* **82**, 064301 (2010).
- [27] J. Q. Chen, *Nucl. Phys. A* **626**, 686 (1997); J. Q. Chen and Y. A. Luo, *ibid.* **639**, 615 (1998); Y. M. Zhao, N. Yoshinaga, S. Yamaji, J. Q. Chen, and A. Arima, *Phys. Rev. C* **62**, 014304 (2000).
- [28] H. Jiang, G. J. Fu, Y. M. Zhao, and A. Arima, *Phys. Rev. C* **84**, 034302 (2011); G. J. Fu, J. J. Shen, Y. M. Zhao, and A. Arima, *ibid.* **87**, 044312 (2013).
- [29] H. Jiang, Y. Lei, G. J. Fu, Y. M. Zhao, and A. Arima, *Phys. Rev. C* **86**, 054304 (2012); H. Jiang, C. Qi, Y. Lei, R. Liotta, R. Wyss, and Y. M. Zhao, *ibid.* **88**, 044332 (2013); H. Jiang, Y. Lei, C. Qi, R. Liotta, R. Wyss, and Y. M. Zhao, *ibid.* **89**, 014320 (2014).
- [30] Y. A. Luo and J. Q. Chen, *Phys. Rev. C* **58**, 589 (1998); L. Y. Jia, H. Zhang, and Y. M. Zhao, *ibid.* **75**, 034307 (2007); **76**, 054305 (2007).
- [31] Z. Y. Xu, Y. Lei, Y. M. Zhao, S. W. Xu, Y. X. Xie, and A. Arima, *Phys. Rev. C* **79**, 054315 (2009); H. Jiang, J. J. Shen, Y. M. Zhao, and A. Arima, *J. Phys. G: Nucl. Part. Phys.* **38**, 045103 (2011).
- [32] Y. M. Zhao and A. Arima, *Phys. Rep.* **545**, 1 (2014).
- [33] <http://www.nndc.bnl.gov/ensdf/>.
- [34] A. Banu *et al.*, *Phys. Rev. C* **72**, 061305(R) (2005).
- [35] A. F. Lisetskiy, N. Pietralla, C. Fransen, R. V. Jolos, and P. von Brentano, *Nucl. Phys. A* **677**, 100 (2000).
- [36] N. J. Stone, *At. Data Nucl. Data Tables* **90**, 75 (2005).
- [37] J. H. Hirata, S. Salém-Vasconcelos, M. J. Bechara, L. C. Gomes, and O. Dietzsch, *Phys. Rev. C* **57**, 76 (1998).
- [38] B. Singh, *Nucl. Data Sheets* **84**, 565 (1998).
- [39] S. Landsberger, R. Lecomte, P. Paradis, and S. Monaro, *Phys. Rev. C* **21**, 588 (1980).
- [40] E. Williams *et al.*, *Phys. Rev. C* **74**, 024302 (2006).
- [41] D. Radeck *et al.*, *Phys. Rev. C* **85**, 014301 (2012).
- [42] R. B. Cakirli *et al.*, *Phys. Rev. C* **70**, 044312 (2004).
- [43] B. Kharraja *et al.*, *Phys. Rev. C* **61**, 024301 (1999).
- [44] K. Kaneko, Y. Sun, T. Mizusaki, and M. Hasegawa, *Phys. Rev. C* **83**, 014320 (2011).